scientific reports

Check for updates

OPEN

Determination of the solubility of methyldopa in supercritical carbon dioxide for drug delivery applications: thermal analysis

Adil Farooq Wali[1], Sathvik Belagodu Sridhar[2], Sirajunisa Talath[1], Jayachithra Ramakrishna Pillai[1], Javedh Shareef[2], Mullaicharam Bhupathyraaj[3], B. K. Manjunatha Goud[4] & Umme Hani[5]✉

The production of fine particles by green technology like supercritical carbon dioxide requires the assessment of substantial solubility data at high pressures. This study represents the first determination of the solubility of methyldopa in carbon dioxide at pressures and temperatures ranging from 12 to 30 MPa and from 313.2 to 343.2 K, respectively. The mole fractions were obtained under the aforementioned conditions and ranged from 0.805×10^{-5} to 11.345×10^{-5}. Four empirical models (Chrastil, Bartle et al., Mendez-Santiago, & Teja, and Kumar-Johnston) and two equations of state (Peng-Robinson and Soave-Redlich-Kwong) were used to correlate drug solubility. The K-J model demonstrated the highest accuracy, with an AARD of 8.38% and a R^2 value of 0.988. Furthermore, the enthalpy values for the drug in SC-CO_2 were estimated using the Chrastil and Bartle models, resulting in values of 34.35 and 56.87 kJ·mol^{-1}, respectively. The results demonstrate that the SRK more pronounced results than the PR model, with an AARD% of 23.03 and a R^2 value of 0.903 compared to 26.42 and 0.837. The article's conclusions provide a valuable reference for the application of green method in the production of fine particles of methyldopa.

Keywords Supercritical fluid, Solubility, Thermodynamic modeling, Semi-empirical and enthalpy

Abbreviations

PR	PR Peng-Robinson EoS
SCF	Supercritical fluid
SRK	Soave-Redlich-Kwong
$ScCO_2$	Supercritical carbon dioxide
CAS Number	Chemical Abstracts Service Registry Number
ECM-RK	Estevez-Colpas-Muller approach based on the
ECM-PR	Estevez-Colpas-Muller approach based on the

List of symbols

AARD	Average absolute relative deviation
a0-a6	The adjustable parameters
a(T) and b	Energy parameter
C	Concentration of solute [g/cm3].
K	Kelvin
$M_{w:}$	Molecular weight of drug [g/mol]
N	Experimental data point
P	Pressure [MPa]
P_c	Critical pressure

[1]Department of Pharmaceutical Chemistry, RAK College of Pharmacy, RAK Medical and Health Sciences University, Ras Al Khaimah, UAE. [2]Department of Clinical Pharmacy and Pharmacology, RAK College of Pharmacy, RAK Medical and Health Sciences University, Ras Al Khaimah, UAE. [3]College of Pharmacy, National University of Science and Technology, Muscat 130, Oman. [4]RAK College of Medical Sciences, RAK Medical and Health Sciences University, Ras Al Khaimah, UAE. [5] Department of Pharmaceutics, College of Pharmacy, King Khalid University, Abha 62529, Saudi Arabia. ✉email: uahmed@kku.edu.sa

P_{ref}	Reference pressure
P_{sub}	Sublimation pressure
Q	Number of independent variables.
R	Ideal gas constant [bar.cm3/K.mol]
SCF	Supercritical Fluid
T	Temperature [K]
T_c	Critical temperature [K]
v	Volume of the sample loop [cm3]
y_2	Solubility of drug in SCF
y_2' :	Drug solubility in ternary system

Greek letter

λ	Wavelength absorbance
ρ	Density [g/cm3]
ΔH	enthalpy
ω	Acentric factor

Subscripts

CO_2	Carbon dioxide
Sol	Solvation
vap	Vaporization

The term "bioavailability" is employed to describe the rate and extent to which a pharmaceutical agent is absorbed and becomes available at the site of action[1]. In the event of insufficient absorption of a pharmaceutical agent, an increase in dosage via oral administration may be a viable option. Such outcomes may give rise to economic challenges, heightened risks of undesirable effects, and unanticipated responses. Moreover, enhancing the availability of pharmaceutical agents can be accomplished by reducing the particle size[2–5]. The conventional methods of evaporation[6], cryogenic spraying[7], crystal engineering[8], recrystallization from solution, and milling[9]have the potential to reduce the size of particles. The application of supercritical fluids represents a novel approach to particle size engineering, which is now being employed by relevant industry[10,1112131415].

The utilization of carbon dioxide as a supercritical fluid in clean technologies enables the generation of minute, homogeneous particles. It is employed as a solvent in a multitude of applications, including extraction and particle formation. $ScCO_2$ possesses distinctive properties due to its relatively low temperature and moderate pressure. CO_2 displays a number of distinctive properties, including cost-effectiveness, ease of removal, non-toxicity, and non-flammability[16–22]. The solubility characteristics of the substance in CO_2 play an important role in the selection and design of supercritical fluid processes, as it identifies the role of CO_2as a solvent and antisolvent for the production of fine particles of the substance. Many research groups have investigated the solubility of various drugs in supercritical carbon dioxide. This research has led to the production of smaller, more uniform drugs with improved dissolution rates[23–30].

The process of testing substance solubility in CO_2 is both expensive and requires a considerable investment of time, representing a significant commitment of resources. Some models including empirical or semi-empirical correlations, equations of state (including cubic and non-cubic models) and intelligent computational techniques (such as artificial neural networks and machine learning methods) have been developed which establish a correlation between solubility at supercritical conditions and make predictions[31–34]. Models founded upon the principles of equations of state inevitably require the estimation of thermodynamic parameters[35–42]. Alternative models (e.g., Garlapati – Madras[43], Reddy-Madras[44], Keshmiri et al.[45]. , , Sparks et al.[46]. , , Chrastil[47], Bartle et al.[48]. , K-J[49], MST[50,51], Del Valle and Aguilera[52], González et al.[53]). have been developed to address this challenge, including those based on empirical evidence, theoretical principles, and the relationship between solute solubility with density, pressure and temperature. These models integrate experimental solubility data with the density of the supercritical solvent, thereby providing a means of integrating empirical data with theoretical principles. The primary distinctions between density-based models pertain to the number of adjusted parameters and the correlation between solubility and density.

The regular solution models are employed to establish correlations between the solubility of compounds in CO_2[54]. In these models, $ScCO_2$ is regarded as a liquid solvent. The non-ideal behavior of solid-liquid equilibrium is taken into account by applying an infinite dilution activity coefficient. An effective approach for correlating the solubility of biological and pharmaceutical compounds is the incorporation of a Flory-Huggins term into a regular solution model[55–63].

Previous studies have not yet reported the solubility of methyldopa in $ScCO_2$; therefore, this investigation aims to fill this gap in the existing literature. The objective of this study is to examine the solubility of methyldopa in $ScCO_2$ at varying temperatures and pressures. The data were correlated using a range of semi-empirical models developed for a binary system ($ScCO_2$ + methyldopa). Furthermore, the data were subjected to thermodynamic modeling techniques, including the Peng-Robinson equation, and the Soave Redlich Kwong. To ensure the reliability of the results, the accuracy of the models was assessed using robust statistical techniques.

Material and method

Material

Methyldopa (CAS Number 41372-08-1), 99.0% pure, was procured from Sigma-Aldrich, Germany. The CO_2 utilized in this investigation was 99.99% pure and was obtained from a local supplier in Abha, Saudi Arabia.

Methods

Supercritical fluid method

Two methods have been employed for the determination of the effectiveness of drug solubility in SCF. The initial series of experiments employs a saturated solution to quantify solubility. This can be achieved through either static or dynamic methodologies. The second category of techniques is contingent upon the methodology employed to analyze the saturated solution. There are four principal categories: gravimetric, spectrometric, chromatographic, and miscellaneous[48]. In this study, a gravimetric method was employed to examine solubility in a laboratory setup according to the procedure reported in previous articles[64,65].

In this study, the solubility of the drug was determined through a static method in conjunction with a gravimetric method, utilizing an apparatus designed for pressures of 40 MPa at 473 K. In this context, the equilibrium cell volume was considered to be 100 ml. The following procedure was used for the measurement: To introduce CO_2 to the solubility cell an automatic pump was used. The pressure within the cell was gauged in increments of 0.1 MPa up to a maximum of 45 MPa.

Once the requisite pressure of CO_2 had been achieved, the flow into the cell was permitted. The cell pressure was monitored by means of a calibrated pressure indicator, which had been calibrated prior to the commencement of the study. A precision thermometer was employed to regulate the system temperature at the specified value through the implementation of a proportional-integral-derivative control method, with a resolution of 1 K. Two grams of the drug were compressed into small tablets, with a diameter of 6 mm. The tablets were then subjected to a five-hour contact process with $ScCO_2$ at a fixed pressure and temperature, with a stirring rate of 200 rpm. To ensure that equilibrium was attained, the equilibrium cell was subjected to a series of gradual, oscillating movements. Subsequently, the equilibrium cell underwent rapid depressurization to reach ambient conditions, after which the residual drug mass was weighed to the precision of 0.01 mg using an analytical balance. The drug mole fraction was then calculated using the following equation, which employs the initial and final drug masses.

$$\mathrm{m_e} = \mathrm{m_i} - \mathrm{m_f} \tag{1}$$

$$\text{Mole of drug} = \frac{\mathrm{m_e}}{\mathrm{M_{w,drug}}} \tag{2}$$

$$y_2 = \frac{\text{Mole of Drug}}{(\text{Mole of drug} + \text{Mole of } CO_2)} \tag{3}$$

$$S = \frac{\rho \times M_{solute} \times y_2}{M_{CO_2} \times (1 - y_2)}. \tag{4}$$

Modeling Framework

The process of measuring the rate of solubility of substances in $ScCO_2$ at varying temperatures and pressures is both time-consuming and costly, due to the necessity of employing a lengthy and costly experimental procedure. The development of appropriate models is a crucial step in the prediction of solubilities. Semi-empirical models are relatively straightforward and are employed for the purpose of forecasting the extent to which substances dissolve in supercritical fluids. A notable number of these models have been developed on the foundation of theoretical models proposed by K-J[49], MST[50], Bartle et al.[48]and Chrastil[47]. Moreover, a number of additional models have been proposed based exclusively on curve fitting and the interrelationships between temperature, pressure, and density with solubility. To provide a comprehensive description of the experimental data, four models that are widely regarded as authoritative in their respective fields have been selected for analysis.

a) Chrastil model[47].

In summary, the Chrastil model established a correlation between the solubility of a solute in SCF and the supercritical fluid density and absolute temperature. The model thus yields the result that a molecule of the solute A forms a complex with K molecules of the solvent B. In this model, the parameters a_0, a_1, and a_2 are adjustable and can be obtained from solubility data. The parameter a_2 is a function of the total heat ($a_2 = \frac{\Delta H_t}{R}$, where R is the universal gas constant and ΔH_t is the sum of vaporization (ΔH_{vap}) and solvation (ΔH_{sol}) enthalpies of the solid solute drug).

$$Ln\ S = a_0 \ln\rho + a_1 + \frac{a_2}{T} \tag{4}$$

b) Bartle et al.[48].

In the study conducted by Bartle et al., the parameter a_2 can be employed to calculate the heat of vaporization of the solute, ΔH_{vap}. Given the values of ΔH_t and ΔH_{vap}, the heat of solvation, ΔH_{sol}, can be approximated for different solute-CO_2 systems.

$$\ln\left(\frac{y_2 P}{P_{ref}}\right) = a_0 + \frac{a_1}{T} + a_2\left(\rho - \rho_{ref}\right) \tag{6}$$

c) Kumar- Johnston[49].

Additionally, in 1988 Kumar and Johnston presented a density-based semi-empirical model that parameters a_0 and a_1 are acquired from empirical data and while the parameter a_2 is related to ΔH_t via $\Delta H_t = \frac{a_2}{R}$.

$$\ln(y_2) = a_0 + a_1\rho + \frac{a_2}{T} \tag{7}$$

d) Mendez-Santiago and Teja[51].

In further model, based on the theory of dilute solutions, MST extended the linear correlation between the solubility of solids in a SCF to encompass a wider range of constants. This was achieved by establishing a linear communication between experimental data and the aforementioned equation.

$$Tln(y_2P) = a_0 + a_1\rho + a_2T \tag{8}$$

As well as, a plethora of models based on phase equilibria have been developed with the objective of establishing correlations between the solubilities of API in CO_2. These encompass models for pharmaceutical compounds in $ScCO_2$ that have been constructed using a range of models. Engineers frequently employ equations of state to predict fluid properties and to elucidate the behavior of mixtures at varying temperatures and pressures. In this field of study, two equations of state (EoSs) were employed, including the PR, and SRK. As previously stated, a thermodynamic study of the API solubility in supercritical carbon dioxide using EoSs requires the calculation of specific API properties through the utilization of appropriate methodologies. The aforementioned parameters include the critical pressure, critical temperature, melting point, boiling point, molar volume, acentric factor, and sublimation vapor pressure. In order to calculate the melting point and boiling point, the Marrero and Gani[66]method was employed. In accordance with the method proposed by Klincewicz[67], the critical pressure and critical temperature of the active substance were calculated. The acentric factor and sublimation vapor pressure were determined using the group contribution method, as proposed by Ambrose Walton and Gani Watson[68]. As demonstrated in Table 1, a variety of techniques were employed in numerous articles for the estimation of these parameters. To describe the solubility data, the PR and SRK models, which are commonly used, have been selected.

a) SRK equation [45]:

$$P = \frac{RT}{v-b} - \frac{a(T)}{v(v+b)}, \tag{9}$$

$$a(T) = \frac{0.42748R^2T_c^2}{P_c} \times \alpha\ (T_r, \omega)\ , \tag{10}$$

$$\alpha\ (T_r, \omega) = \left[1 + m\left(1 - T_r^{0.5}\right)\right]^2, \tag{11}$$

$$m = 0.480 + 1.574\omega\ - 0.176\omega^{\ 2}, \text{ and} \tag{12}$$

$$b = \frac{0.08664RT_c}{P_c}. \tag{13}$$

b) PR equation [46]:

$$P = \frac{RT}{v-b} - \frac{a(T)}{v(v+b) + b(v-b)}\ , \tag{14}$$

$$a(T) = \frac{0.45724R^2T_c^2}{P_c} \times \alpha\ (T_r, \omega)\ , \tag{15}$$

$$\alpha\ (T_r, \omega) = \left[1 + k\left(1 - T_r^{0.5}\right)\right]^2, \tag{16}$$

$$k = 0.37464 + 1.54226\omega\ - 0.26992\omega^{\ 2}, \text{ and} \tag{17}$$

$$b = \frac{0.07780RT_c}{P_c}\ . \tag{18}$$

Results and discussion

Methyldopa solubility in ScCO2

The aim of this study was to gain insight into the solubility of methyldopa that could be dissolved in supercritical carbon dioxide at varying pressures (12–30 MPa) and temperatures (313–343 K). The details of the experimental conditions and the CO_2 density, along with the resulting outcomes, can be found in Table 2. The data points report the mean of at least three times. The density of CO_2 was sourced from the NIST Chemistry[96]. The API solubility, S, and mole fraction, y, exhibited a range of 8.05×10^{-6} to 1.13×10^{-5} and 0.0134 to 0.4279 g/L, respectively. As illustrated in Table 2, the standard deviation of the solubility results is less than 4.5%. To examine the effect of temperature and pressure in a simultaneous manner, Fig. 1a and b have been created in three dimensions. As depicted in Fig. 1a, the drug solubility in $ScCO_2$ demonstrated an increase with pressure. In addition, as illustrated in Table 2, an increase in pressure is accompanied by a corresponding rise in the molar fraction value. At 313 K, the value rises from 2.481×10^{-5} to 7.652×10^{-5}. At 323 K, it increases from 1.880×10^{-5} to 8.832×10^{-5}. At 333 K, the molar fraction value increased from 1.520×10^{-5} to 9.960×10^{-5}. At 343 K, it increased from 0.805×10^{-5} to 11.345×10^{-5}. This phenomenon can be attributed to the rise in CO_2 density and solvating power, which

No	Drug	Eos	v	ω	T_c	P_c	References
1.	n-(4-Ethoxyphenyl)ethanamide	PR	157.1	0.70	700.3	33.29	
2.	Lauric	PR	-	0.9135	797.6	19.22	69
3.	Myristic	PR	-	0.9612	841.6	16.35	69
4.	Palmitic	PR	-	0.9846	887.3	14.08	69
5.	Stearic	PR	-	0.9786	935.1	12.25	69
1.	Behenic	PR	-	0.8685	1038.7	9.52	69
2.	Sodium Valproate	SRK, PR, SAFT-VR	148.4[g]	0.41[i]	612.92[a]	25.83[a]	42
3.	Sorafenib tosylate	SRK, PR, with vdW2 and Wong-Sandler	387.5[g]	0.392[d]	1087.90[a]	15.496[a]	70
4.	Minoxidil	SRK, PR, combined with either Wong-Sandler or van der Waals	141.1[c]	0.7[i]	879.6[a]	35.56[a]	71
5.	Chlorothiazide	PR-EoS	369.20[c]	0.62[b]	933.24[a]	45.85[a]	72
6.	Repaglinide	PR, and UNIQUAC	257.5[g]	0.352[d]	938.026[a]	11.672[a]	73
7.	Imatinib mesylate	SRK, Pazuki et al. (PAZ), and Haghtalab et al. (HKM) with dW2	412.5[g]	0.450[d]	1000.24[a]	15.477[a]	74
8.	Esomeprazole	SRK, combined with Renon mixing rule	214.2[g]	1.29[j]	979.36[e]	25.00[e]	40
9.	Aprepitant	SRK, PR	351.3[g]	1.14[i]	823[h]	10.38[h]	75
10.	Lacosamide	PR-EoS with vdW2 mixing rule and PC-SAFT	220.06[c]	1.1399[d]	968.86[e]	2.5[e]	76
11.	1-aminoanthraquinone	Regular solution model and PRSV-EoS	117.6[g]	0.853i	928	3.142	77
12.	1-nitroanthraquinone	Regular solution model and PRSV-EoS	155.4[g]	0.921[i]	916	2.836	77
13.	Glibenclamide	PR-EoS with vdW2	374.47[c]	1.4772[d]	1443.97[e]	1.8055[e]	78
14.	Tamsulosin	SAFT-VR and Peng-Robinson (PR)	375.8[g]	0.627[d]	999.846[a]	1.3871[a]	79
15.	Fludrocortisone acetate	PC-SAFT	337.1[c]	0.7[b]	947.4[a]	17.42[a]	80
16.	Famotidine	PC-SAFT, and e Estevez et al. model (ECM-PR and ECM-RK)	358.1[c]	0.991[b]	901.46 [a]	43.50[a]	81
17.	Chloroquine	SRK, PR, modified Wilson's and UNIQUAC	209.3[c]	0.47[b]	917[a]	16.5[a]	34
18.	Lenalidomide	SRK with two parameters van der Waals (vdW2) (modified Wilson's model)	166.40[c]	0.64[b]	1006.12[a]	36.54[a]	82
19.	Favipiravir	SRK with quadratic mixing rules	97.53[c]	0.5799[d]	878.71[a]	66.82[a]	83
20.	Aripiprazole	modified Wilson	552.8[c]	0.3189[d]	981.18[a]	6.07[a]	84
21.	Dapagliflozin propanediol monohydrate	PR-EoS d with van der Waals	310.12[g]	0.5307[d]	985.056[a]	14.4[a]	85
22.	Mebeverine Hydrochloride	SRK, PR, and Estévez et al. models	387.5[c]	0.6773[i]	1066[k]	15.6[k]	86
23.	Sildenafil citrate	SRK, PC-SAFT and Modified Wilson model.	460.9[c]	1.78[d]	1058.8[a]	17.64[a]	87
24.	Coumarin-7	qCPA-PCPSAFT	170.9[a]	1.37[b]	919.76[a]	23.66[a]	88
25.	Gemiflxacin	SRK and PR, and the regular solution model	445[c]	1.04[i]	1012.50[a]	1012.50[a]	20
26.	Nifedipine	PR	235.9[g]	0.6487[j]	871.7[e]	19.33[e]	89
27.	Lacidipine	PR	362.4[g]	0.6225[j]	950.8[e]	12.93[e]	89
28.	Squalene	GC-EOS	-	2.32	716.5[b]	7.19[b]	90

Table 1. Summary of the method applied to estimate properties of substances. a Calculated using Marrero and Gani Method[66]. b Constantinou – Gani[68]. c Immirzi–Perini method[91]. d Ambrose–Walton[92], e Joback method[68], f Grain-Watson method[93], g Fedors'method[94], h Wilson–Jasperson[68], i Edmister method[68], j Lee-Kesler method[95], K Klincewicz-Reid method[67] .

enhance solute-solvent interactions by reducing the mean intermolecular distance, thereby facilitating greater solubility. As indicated in Table 2, the solubility data yielded minimum and maximum values at 343 K, which points to the potential existence of a crossover pressure within the system. Furthermore, Fig. 1a clearly illustrates the varying trends evident in the isotherms, indicated by their different slopes and the crossover at a pressure of approximately between 16 and 18 MPa. This phenomenon is undoubtedly attributable to the opposing effects of temperature on the two variables that influence solubility: API sublimation vapor pressure, and CO_2 density. The greatest impact on density was observed in the region below the crossover region. At pressures above the crossover point, the sublimation vapor pressure was identified as the dominant factor. The solvent exhibits diminished sensitivity to pressure, which consequently results in augmented solubility at elevated temperatures. The solubility of drugs in SC-CO_2 is influenced by temperature, as changes in temperature alter the density of CO_2 and the sublimation vapor pressure of the drug. Guo et al. (2018) measured the solubility of cinnamic acid in supercritical carbon dioxide at temperatures from 308 to 328 K and pressures of 9.0 to 18.0 MPa. They explained how temperature affects solubility in the crossover region (11 to 13 MPa)[97]. Pishnamazi et al. (2020) also studied the solubility of tamoxifen at different pressures and temperatures. Tamoxifen is affected by pressure and temperature. Pressure affects solubility directly, while temperature depends on the crossover pressure, which is about 200 bar for tamoxifen. For pressures above the crossover point, increasing temperature enhances tamoxifen solubility due to sublimation pressure. For pressures below the crossover point, density reduction is

T (K)[a]	*P* (MPa)	ρ (kg.m^{-3})	y × 10^5	SD (ȳ) × 10^4	Solubility (g/L)
313	12	719.2	2.481	0.013	0.0856
	15	781.2	3.013	0.018	0.1128
	18	820.7	3.942	0.020	0.1551
	21	850.4	4.531	0.022	0.1848
	24	873.9	5.520	0.030	0.2313
	27	893.5	6.320	0.033	0.2709
	30	910.3	7.652	0.034	0.3342
323	12	587.2	1.880	0.012	0.0530
	15	701.1	3.390	0.021	0.1141
	18	758.8	4.490	0.025	0.1634
	21	797.4	5.910	0.033	0.2261
	24	826.1	7.114	0.041	0.2819
	27	851.7	7.790	0.033	0.3182
	30	871.5	8.832	0.041	0.3692
333	12	435.3	1.520	0.010	0.0317
	15	606.8	2.841	0.018	0.0826
	18	688.4	5.090	0.030	0.1681
	21	740.3	7.050	0.033	0.2504
	24	777.5	8.125	0.040	0.3029
	27	806.7	9.163	0.032	0.3544
	30	830.5	9.960	0.055	0.3968
343	12	346.1	0.805	0.010	0.0134
	15	507.5	2.043	0.011	0.0497
	18	613.5	5.410	0.023	0.1593
	21	678.9	7.484	0.036	0.2438
	24	724.9	8.632	0.051	0.3003
	27	760.3	10.061	0.060	0.3672
	30	788.9	11.345	0.065	0.4279

Table 2. Solubility and mole fraction of methyldopa.

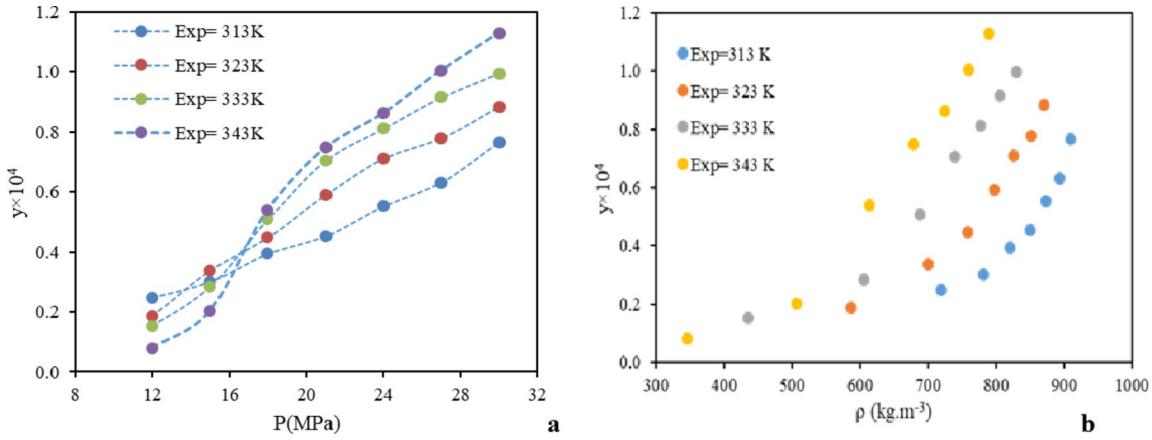

Fig. 1. Experimental mole fraction of Methyldopa in $ScCO_2$ (**a**) based on pressure and (**b**) density of CO_2.

the dominant mechanism as temperature rises[98]. Similar results were reported for busulfan[99]and chloroquine[100]. Moreover, Ongkasin et al. (2019) found that solubility changes with temperature because of two opposing effects. As temperature rises, CO_2density falls and solute vapor pressure rises. At 25 MPa, density is the main factor, but at higher pressures, vapor pressure is the main factor, increasing solubility with rising temperature[101].

Semi-empirical models

In order to evaluate the consistency of the binary solubility data, four models were utilized. These models were used to correlate many solutes. These correlations don't need extra properties. Two criteria were used to compare the models. AARD and R_{adj}.

$$AARD\% = \frac{1}{N}\sum_{i=1}^{n}\left(\left|\frac{y_{i,cal} - y_{i,exp}}{y_{i,exp}}\right|\right) \times 100\,\%$$

$$R^2 = 1 - \frac{\sum_{n=1}^{N}(y_n^{exp} - y_n^{calc})^2}{\sum_{n=1}^{N}(y_n^{exp} - \overline{y})^2}$$

The AARD of Chrastil, Bartle, K-J and MST's models were achieved 09.70, 11.07, 8.38, and 10.19. K-J model with three adjustable parameters worked well for solubility data. Figure 2a-d shows the correlation results and the consistency of supercritical CO_2-solid solubility data, self-consistency tests were conducted using the four models. To achieve this objective, the experimental data were subjected to a linear regression analysis with the aim of obtaining a linear correlation for the solubility data when employing each model. The linearity of the data permits an evaluation of its self-consistency. Subsequently, the correlation coefficients (R^2) obtained for all four semi-empirical methods, including MST (0.975), Bartle et al. (0.958), K-J (0.988), and Chrastil (0.987), were deemed indicative of the method with the greatest capacity for extrapolation (Table 3). Méndez-Santiago &Teja[50] proposed an expression based on the theory of dilute solutions to correlate the solubility of a wide range of solids in supercritical carbon dioxide.

The linear trend was demonstrated to be applicable across a broad range of temperatures, with the exception of densities below approximately half the critical density of CO_2 as a solvent.

The linear relationships presented in this study facilitate the extrapolation of solubility over a range of temperatures. Moreover, the relationship provides a means of verifying the consistency of solubility data. This model was employed by numerous researchers (Shojaee et al.[102]; Tamura et al.[77]; Sabegh et al.[103]) to assess the consistency of experimental data. This was achieved by plotting the quantity $T(\ln(y.P) - X_3)$ versus density ρ, which should yield a straight line if the data are consistent. An example of this is illustrated in Fig. 2d.

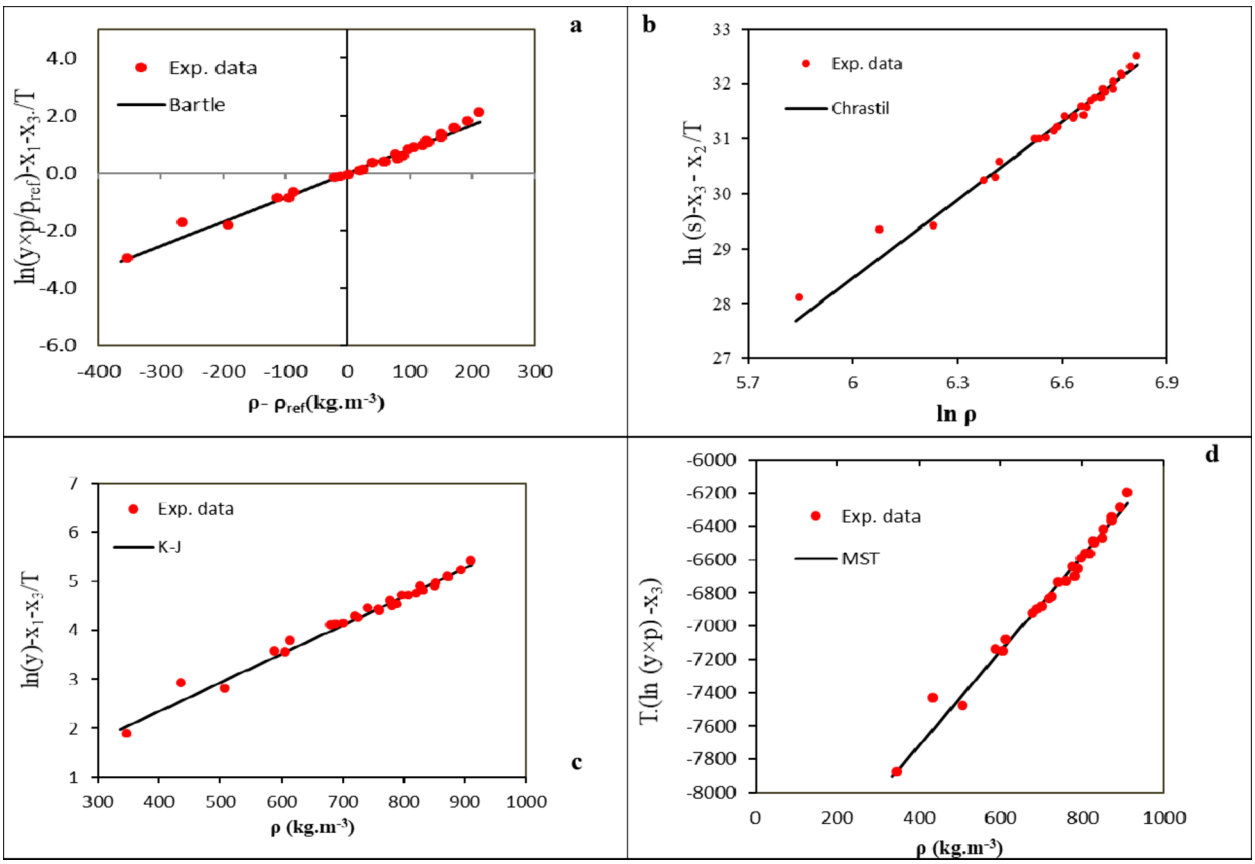

Fig. 2. Self-consistency test for methyldopa solubility in supercritical carbon dioxide **(a)** Bartle et al. **(b)** Chrastil et al. **(c)** K-J **(d)** MST.

Models	Parameters			Criteria	
	a	b	c	AARD (%)	R^2
Chrastil	4.71	−20.20	−4132.3	09.70	0.987
Bartle	0.0084	15.94	−6840.2	11.07	0.958
K-J	−0.195	0.0059	−4605	08.38	0.988
MST	13.7	2.80	−8857.8	10.19	0.975

Table 3. The outcome of the density based models.

Component	Boiling point (K)	Critical temperature (K)	Critical pressure (MPa)	Acentric factor	Molar volume (cm^3/mol)
Methyldopa	981.3[a]	1395.7[a]	2.45[a]	0.558[b]	335.4[c]
P^{sub} (Pa) [d]					
	1.96×10^{-9} (313 K)	1.35×10^{-8} (323 K)	8.17×10^{-8} (333 K)	4.37×10^{-7} (343 K)	

Table 4. Properties of methyldopa.

Model	Parameter	T = 313 K	T = 323 K	T = 333 K	T = 343 K	Overall
PR- vdW2	k_{12}	−0.3957	−0.4380	−0.4590	−0.5674	
	l_{12}	−0.5945	−0.6777	−0.7152	−0.9467	
	$AARD$	16.01	21.50	33.11	35.09	26.42
	R_{adj}	0.8699	0.8589	0.8170	0.8005	0.837
SRK	k_{12}	−0.2911	−0.3703	−0.4457	−0.9016	
	l_{12}	−0.3875	−0.5499	−0.7123	−0.5384	
	$AARD$	23.05	16.23	24.98	27.87	23.03
	R_{adj}	0.9017	0.9386	0.8906	0.8795	0.903

Table 5. Results for solubility of methyldopa in $ScCO_2$, by PR and SRK.

Nasri[104] presented two steps: a review of the estimation of the Krichevskii parameter and a second step of estimating sublimation enthalpy and sublimation pressure. For both thermophysical properties, the dilute solution theory was adopted in a new way based on the consistency of solid solubility data in supercritical carbon dioxide.

The discrepancy in results can be attributed to the incorporation of an energy term (specifically, the temperature term's coefficient) into the Chrastil, K-J and Bartle et al. The overall reaction and vaporization enthalpy of the substance under examination are contingent upon two adjustable parameters: a_2 from Chrastil and Bartle's model.

This allowed for the evaluation of the total heat (ΔH_{total}), vaporization heat (ΔH_{vap}), and solvation heat (ΔH_{sol}) of the examined methyldopa-CO_2 systems based on the regressed energy parameters. The difference between the vaporization heat (ΔH_{vap}) as defined by the Bartle et al. model and the total reaction heat (ΔH_{total}) as defined by Chrastil's model was considered to be the solvation heat (ΔH_{sol}). The enthalpy values for methyldopa in $ScCO_2$ as determined by the Chrastil and Bartle models are 34.35 and 56.87 kJ·mol^{-1}, respectively. Given the endothermic nature of vaporization, in contrast with the exothermic character of solvation, the heat released during the vaporization process exceeded the total amount of heat absorbed. When evaluated as the discrepancy between the vaporization heat (ΔH_{vap}) and the total reaction heat (ΔH_{total}), the solvation heat (ΔH_{sol}) was determined to be −22.52 kJ/mol.

Equation of state

As previously stated, the equations of state can be utilized only after the requisite parameters have been calculated. As indicated in Table 4, the boiling temperature (981.3 K) was calculated using the Marrero and Gani's formula[66], the critical temperature (1395.7 K) and pressure (2.45 MPa) were calculated using the the Marrero and Gani's correlation[66], the molar volume (335.3 cm^3/mol) was calculated using the Immirzi–Perini method[91], the eccentric factor (0.558) was calculated using the Ambrose–Walton corresponding states method[92], and the sublimation vapor pressure (1.96×10^{-9} (313 K), 1.35×10^{-8} (323 K), 8.17×10^{-8} (333 K), and 4.37×10^{-7}(343 K)) was calculated using the Grain-Watson method[93]. As reported in Table 1, several articles employed various methods for estimating these parameters.

Table 5 illustrate results of the correlation between EoSs with Vander Waals mixing rule with two interaction parameters (vdW2) at temperatures of 313, 323, 333 and 343. As illustrated in Table 5, the SRK with the vdW2 mixing rule exhibits the most pronounced outcomes, with an AARD% of 23.03 and an R^2value of 0.903, in comparison with PR, which displays an AARD% of 26.42 and an R^2 value of 0.837.

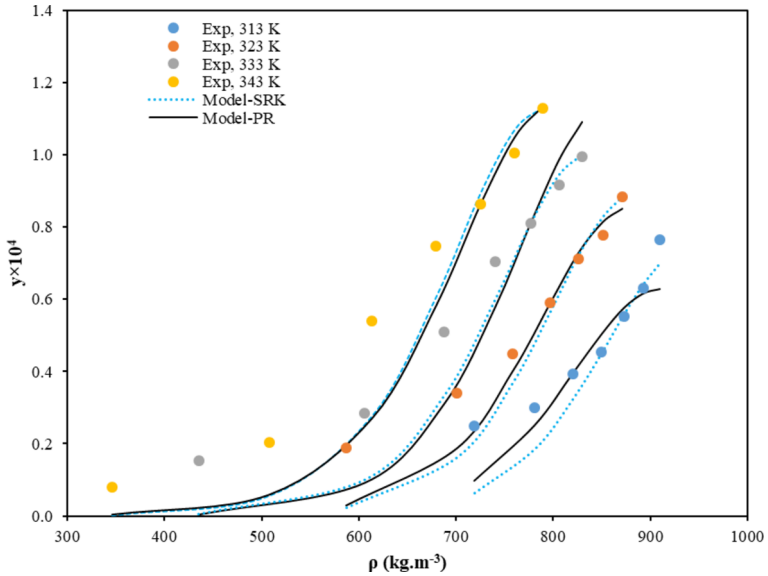

Fig. 3. Results of equations of state modeling.

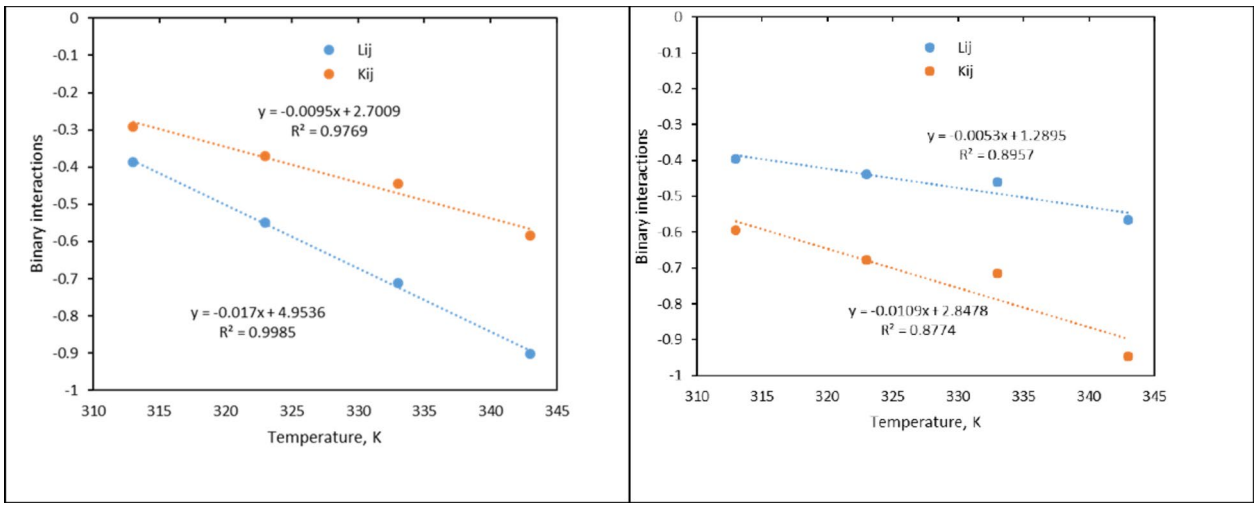

Fig. 4. Interaction parameters of mixing rule for SRK and PR.

The outcomes of the PR and SRK models exhibited a precise correlation between methyldopa solubility in $ScCO_2$ at temperatures between 313 and 343 K. The data indicate a strong correlation between experimental and calculated solubility values at four temperatures using the PR-vdW2 and SRK-vdW2 models (Fig. 3a and b). Nevertheless, at elevated temperatures, a slight divergence from the optimal correlation was observed. Conversely, the correlation of the PR and SRK estimates exhibits minimal error at low temperatures. Nevertheless, at elevated temperatures, the discrepancies increase. These findings are consistent with those of other investigations (Coimbra et al.[105]; Huang et al.[106].; Khimeche et al.[107]).

Figure 4a, and b demonstrate that the parameters for the mixing rule (k_{ij} and l_{ij}) exhibit a linear relationship with temperature.

$$k_{ij} = AT + B \tag{12}$$

$$l_{ij} = AT + B \tag{13}$$

The interaction parameters (k_{ij} and l_{ij}) are utilized to examine the parameters of the PR and SRK for methyldopa-CO_2. The k_{ij} and l_{ij}, AARD%, and Radj values can be calculated and are presented in Table 5 for reference. The PR-dependently adjustable parameters (k_{ij} and l_{ij}) are subject to temperature-dependent variation. The k_{ij} and l_{ij} parameters exhibit a negative correlation with temperature. The solubilities of methyldopa on PR and SRK with vdW2 mixing rules based on EoS were calculated and illustrated in Fig. 4a and b, respectively. Furthermore, the

figures illustrate the impact of temperature on the interaction parameters. As demonstrated in Table 5; Fig. 4, the PR and SRK model's parameters are all negative. Four parameters, designated A, B, C, and D, were subjected to linear regression analysis in accordance with the specifications set forth in Eqs. (12) and (13) and illustrated in Fig. 4.

Conclusion

The capacity to determine the extent of solubility of substances in supercritical fluids represents a crucial element in the synthesis of nanoparticles. The objective of this study was to examine the solubility of methyldopa in supercritical carbon dioxide at varying pressures and temperatures. The solubility data exhibited a range of 0.805×10^{-5} to 11.345×10^{-5}. The highest solubility (0.4279 g/L) was observed at 30 MPa and 343.2 K. Two groups of models were employed, including equation of state and density-based models. In order to assess solute solubility in CO_2 with density-based models, four models were employed: the Chrastil, Bartle et al., K-J, and MST models. The K-J model exhibited the highest degree of accuracy, with an AARD of 8.38% and R^2value of 0.988. The results illustrates that the SRK model with the vdW2 mixing rule produce the most notable outcomes, with an AARD% of 23.03 and R^2value of 0.903, in comparison with the PR model, which displays an AARD% of 26.42 and R^2 value of 0.837. The results obtained in this research show the path of using the supercritical process to produce nanoparticles, and in future work, these data can be used to produce micro and nano particles.

Data availability

The datasets used and analysed during the current study are available from the corresponding author (Umme Hani) on reasonable request.

Received: 17 November 2024; Accepted: 23 December 2024
Published online: 06 January 2025

References

1. Brunton, L. L., Knollmann, B. C. & Hilal-Dandan, R. *Goodman & Gilman's the pharmacological basis of therapeutics* (McGraw Hill Medical New York, 2018).
2. Amidon, G. L., Lennernäs, H., Shah, V. P. & Crison, J. R. A theoretical basis for a biopharmaceutic drug classification: the correlation of in vitro drug product dissolution and in vivo bioavailability. *Pharm. Res.* **12**, 413–420 (1995).
3. Agoram, B., Woltosz, W. S. & Bolger, M. B. Predicting the impact of physiological and biochemical processes on oral drug bioavailability. *Adv. Drug Deliv. Rev.* **50**, S41–S67 (2001).
4. Krishnaiah, Y. S. Pharmaceutical technologies for enhancing oral bioavailability of poorly soluble drugs. *J. Bioequiv Availab.* **2**, 28–36 (2010).
5. Zeng, M. et al. The integration of nanomedicine with traditional Chinese medicine: drug delivery of natural products and other opportunities. *Mol. Pharm.* **20**, 886–904 (2022).
6. Villicaña-Molina, E., Pacheco-Contreras, E., Aguilar-Reyes, E. A. & León-Patiño, C. A. Pectin and chitosan microsphere preparation via a water/oil emulsion and solvent evaporation method for drug delivery. *Int. J. Polym. Mater. Polym. Biomaterials.* **69**, 467–475 (2020).
7. Sahakijpijarn, S., Moon, C. & Williams, R. O. III in *Formulating Poorly Water Soluble Drugs* 453–528Springer, (2022).
8. Bolla, G., Sarma, B. & Nangia, A. K. Crystal engineering of pharmaceutical cocrystals in the discovery and development of improved drugs. *Chem. Rev.* **122**, 11514–11603 (2022).
9. Paredes, A. J. et al. Ricobendazole nanocrystals obtained by media milling and spray drying: pharmacokinetic comparison with the micronized form of the drug. *Int. J. Pharm.* **585**, 119501 (2020).
10. Hao, X. et al. Nanomaterials for bone metastasis. *J. Controlled Release*. **373**, 640–651 (2024).
11. Serajuddin, A. T. Solid dispersion of poorly water-soluble drugs: early promises, subsequent problems, and recent breakthroughs. *J. Pharm. Sci.* **88**, 1058–1066 (1999).
12. Türk, M. & Bolten, D. Formation of submicron poorly water-soluble drugs by rapid expansion of supercritical solution (RESS): results for naproxen. *J. Supercrit. Fluids*. **55**, 778–785 (2010).
13. Junyaprasert, V. B. & Morakul, B. Nanocrystals for enhancement of oral bioavailability of poorly water-soluble drugs. *Asian J. Pharm. Sci.* **10**, 13–23. https://doi.org/10.1016/j.ajps.2014.08.005 (2015).
14. Esfandiari, N. & Sajadian, S. A. CO2 utilization as Gas Antisolvent for the Pharmaceutical Micro and Nanoparticle production: a review. *Arab. J. Chem.*, **104164** (2022).
15. Chen, W. et al. In situ Engineering of Tumor-Associated macrophages via a Nanodrug-Delivering-Drug (β-Elemene@ Stanene) strategy for enhanced Cancer Chemo-Immunotherapy. *Angew. Chem. Int. Ed.* **62**, e202308413 (2023).
16. Kankala, R. K., Xu, P. Y., Chen, B. Q., Wang, S. B. & Chen, A. Z. Supercritical fluid (SCF)-assisted fabrication of carrier-free drugs: an eco-friendly welcome to active Pharmaceutical ingredients (APIs). *Adv. Drug Deliv. Rev.*, **113846** (2021).
17. Franco, P. & De Marco, I. Nanoparticles and nanocrystals by supercritical CO2-assisted techniques for pharmaceutical applications: a review. *Appl. Sci.* **11**, 1476 (2021).
18. Champeau, M., Thomassin, J. M., Tassaing, T. & Jérôme, C. Drug loading of polymer implants by supercritical CO2 assisted impregnation: a review. *J. Controlled Release*. **209**, 248–259 (2015).
19. Knez, Ž. et al. Industrial applications of supercritical fluids: a review. *Energy* **77**, 235–243 (2014).
20. Arabgol, F., Amani, M., Ardestani, N. S. & Sajadian, S. A. Experimental and thermodynamic investigation of gemifloxacin solubility in supercritical CO2 for the production of nanoparticles. *J. Supercrit. Fluids*. **206**, 106165 (2024).
21. Sajadian, S. A., Peyrovedin, H., Zomorodian, K. & Khorram, M. Using the supercritical carbon dioxide as the solvent of Nystatin: studying the effect of co-solvent, experimental and correlating. *J. Supercrit. Fluids*. **194**, 105858. https://doi.org/10.1016/j.supflu.2023.105858 (2023).
22. Ansari, E., Honarvar, B., Sajadian, S. A., Aboosadi, Z. A. & Azizi, M. Solubility of Aripiprazole in supercritical carbon dioxide: Experimental and modeling evaluations. (2023).
23. Askarizadeh, M., Esfandiari, N., Honarvar, B., Sajadian, S. A. & Azdarpour, A. Kinetic Modeling to Explain the Release of Medicine from Drug Delivery Systems. *ChemBioEng Reviews*.
24. Sodeifian, G. & Sajadian, S. A. Solubility measurement and preparation of nanoparticles of an anticancer drug (letrozole) using rapid expansion of supercritical solutions with solid cosolvent (RESS-SC). *J. Supercrit. Fluids*. **133**, 239–252 (2018).
25. Sodeifian, G., Sajadian, S. A. & Daneshyan, S. Preparation of Aprepitant nanoparticles (efficient drug for coping with the effects of cancer treatment) by rapid expansion of supercritical solution with solid cosolvent (RESS-SC). *J. Supercrit. Fluids*. **140**, 72–84 (2018).

26. Sodeifian, G., Razmimanesh, F., Sajadian, S. A. & Panah, H. S. Solubility measurement of an antihistamine drug (loratadine) in supercritical carbon dioxide: Assessment of qCPA and PCP-SAFT equations of state. *Fluid. Phase. Equilibria*. **472**, 147–159 (2018).
27. Sodeifian, G. & Sajadian, S. A. Utilization of Ultrasonic-assisted RESOLV with polymeric stabilizers for production of Amiodarone Hydrochloride nanoparticles: optimization of the process parameters. *Chem. Eng. Res. Des*. **142**, 268–284 (2019).
28. Keshavarz, A. et al. Preparation and characterization of raloxifene nanoparticles using rapid expansion of supercritical solution (RESS). *J. Supercrit. Fluids*. **63**, 169–179 (2012).
29. Fattahi, A. et al. Preparation and characterization of simvastatin nanoparticles using rapid expansion of supercritical solution (RESS) with trifluoromethane. *J. Supercrit. Fluids*. **107**, 469–478 (2016).
30. Behjati Rad, H., Sabet, K., Varaminian, F. & J. & Effect of Stearic Acid as a co-solvent on the solubility enhancement of aspirin in supercritical CO2. *Chem. Eng. Technol.* **42**, 1259–1267 (2019).
31. Si-Moussa, C., Belghait, A., Khaouane, L., Hanini, S. & Halilali, A. Novel density-based model for the correlation of solid drugs solubility in supercritical carbon dioxide. *C. R. Chim.* **20**, 559–572 (2017).
32. Bian, X. Q., Zhang, Q., Du, Z. M., Chen, J. & Jaubert, J. N. A five-parameter empirical model for correlating the solubility of solid compounds in supercritical carbon dioxide. *Fluid. Phase. Equilibria*. **411**, 74–80 (2016).
33. Tabaraki, R. & Toulabi, A. Solubility modeling in three supercritical carbon dioxide, ethane and trifluoromethane fluids by one set of molecular descriptors. *Fluid. Phase. Equilibria*. **383**, 108–114 (2014).
34. Ardestani, N. S., Amani, M., Grishina, M. & Shirazian, S. Theoretical and experimental study on Chloroquine drug solubility in supercritical carbon dioxide via the thermodynamic, multi-layer perceptron neural network (MLPNN), and molecular modeling. *Arab. J. Chem.* **15**, 104371 (2022).
35. Haghtalab, A., Kamali, M., Mazloumi, S. H. & Mahmoodi, P. A new three-parameter cubic equation of state for calculation physical properties and vapor–liquid equilibria. *Fluid. Phase. Equilibria*. **293**, 209–218 (2010).
36. Yazdizadeh, M., Eslamimanesh, A. & Esmaeilzadeh, F. Thermodynamic modeling of solubilities of various solid compounds in supercritical carbon dioxide: effects of equations of state and mixing rules. *J. Supercrit Fluids*. **55**, 861–875. https://doi.org/10.1016/j.supflu.2010.10.019 (2011).
37. Hosseini Anvari, M. & Pazuki, G. A study on the predictive capability of the SAFT-VR equation of state for solubility of solids in supercritical CO2. *J. Supercrit. Fluids*. **90**, 73–83. https://doi.org/10.1016/j.supflu.2014.03.005 (2014).
38. Sodeifian, G., Hazaveie, S. M., Sajadian, S. A. & Razmimanesh, F. Experimental investigation and modeling of the solubility of oxcarbazepine (an anticonvulsant agent) in supercritical carbon dioxide. *Fluid. Phase. Equilibria*. **493**, 160–173 (2019).
39. Sodeifian, G., Saadati Ardestani, N. & Sajadian, S. A. Solubility measurement of a pigment (phthalocyanine green) in supercritical carbon dioxide: experimental correlations and thermodynamic modeling. *Fluid. Phase. Equilibria*. **494**, 61–73. https://doi.org/10.1016/j.fluid.2019.04.024 (2019).
40. Sodeifian, G., Derakhsheshpour, R. & Sajadian, S. A. Experimental study and thermodynamic modeling of Esomeprazole (proton-pump inhibitor drug for stomach acid reduction) solubility in supercritical carbon dioxide. *J. Supercrit. Fluids*. **154**, 104606 (2019).
41. Sodeifian, G., Sajadian, S. A. & Derakhsheshpour, R. Experimental measurement and thermodynamic modeling of Lansoprazole solubility in supercritical carbon dioxide: application of SAFT-VR EoS. *Fluid. Phase. Equilibria*. **507**, 112422 (2020).
42. Sodeifian, G., Saadati Ardestani, N., Sajadian, S. A., Golmohammadi, M. R. & Fazlali, A. Prediction of solubility of Sodium Valproate in Supercritical Carbon Dioxide: experimental study and thermodynamic modeling. *J. Chem. Eng. Data*. **65**, 1747–1760 (2020).
43. Garlapati, C. & Madras, G. New empirical expressions to correlate solubilities of solids in supercritical carbon dioxide. *Thermochim Acta*. **500**, 123–127 (2010).
44. Reddy, S. N. & Madras, G. Modeling of ternary solubilities of solids in supercritical carbon dioxide in the presence of cosolvents or cosolutes. *J. Supercrit. Fluids*. **63**, 105–114 (2012).
45. Keshmiri, K., Vatanara, A. & Yamini, Y. Development and evaluation of a new semi-empirical model for correlation of drug solubility in supercritical CO 2. *Fluid. Phase. Equilibria*. **363**, 18–26 (2014).
46. Sparks, D. L., Hernandez, R. & Estévez, L. A. Evaluation of density-based models for the solubility of solids in supercritical carbon dioxide and formulation of a new model. *Chem. Eng. Sci.* **63**, 4292–4301 (2008).
47. Chrastil, J. Solubility of solids and liquids in supercritical gases. *J. Phys. Chem.* **86**, 3016–3021 (1982).
48. Bartle, K., Clifford, A., Jafar, S. & Shilstone, G. Solubilities of solids and liquids of low volatility in supercritical carbon dioxide. *J. Phys. Chem. Ref. Data*. **20**, 713–756 (1991).
49. Kumar, S. K. & Johnston, K. P. Modelling the solubility of solids in supercritical fluids with density as the independent variable. *J. Supercrit. Fluids*. **1**, 15–22 (1988).
50. Méndez-Santiago, J. & Teja, A. S. The solubility of solids in supercritical fluids. *Fluid. Phase. Equilibria*. **158**, 501–510 (1999).
51. Mendez-Santiago, J. & Teja, A. S. Solubility of solids in supercritical fluids: consistency of data and a new model for cosolvent systems. *Ind. Eng. Chem. Res.* **39**, 4767–4771 (2000).
52. Del Valle, J. M. & Aguilera, J. M. An improved equation for predicting the solubility of vegetable oils in supercritical carbon dioxide. *Ind. Eng. Chem. Res.* **27**, 1551–1553 (1988).
53. González, J. C., Vieytes, M. R., Botana, A. M., Vieites, J. M. & Botana, L. M. Modified mass action law-based model to correlate the solubility of solids and liquids in entrained supercritical carbon dioxide. *J. Chromatogr. A*. **910**, 119–125 (2001).
54. Sodeifian, G., Garlapati, C., Razmimanesh, F. & Nateghi, H. Solubility measurement and thermodynamic modeling of pantoprazole sodium sesquihydrate in supercritical carbon dioxide. *Sci. Rep.* **12**, 7758 (2022).
55. Alwi, R. S. et al. Experimental study and thermodynamic modeling of clonazepam solubility in supercritical carbon dioxide. *Fluid. Phase. Equilibria*. **574**, 113880. https://doi.org/10.1016/j.fluid.2023.113880 (2023).
56. Sodeifian, G., Alwi, R. S., Razmimanesh, F. & Abadian, M. Solubility of Dasatinib monohydrate (anticancer drug) in supercritical CO2: experimental and thermodynamic modeling. *J. Mol. Liq.* **346**, 117899 (2022).
57. Sodeifian, G., Alwi, R. S., Razmimanesh, F. & Sodeifian, F. Solubility of prazosin hydrochloride (alpha blocker antihypertensive drug) in supercritical CO2: experimental and thermodynamic modelling. *J. Mol. Liq.* **362**, 119689 (2022).
58. Alwi, R. S. & Garlapati, C. A new semi empirical model for the solubility of dyestuffs in supercritical carbon dioxide. *Chem. Pap.* **75**, 2585–2595. https://doi.org/10.1007/s11696-020-01482-x (2021).
59. Alwi, R. S. & Tamura, K. Measurement and correlation of derivatized anthraquinone solubility in supercritical carbon dioxide. *J. Chem. Eng. Data*. **60**, 3046–3052 (2015).
60. Sodeifian, G., Nasri, L., Razmimanesh, F. & Nooshabadi, M. A. Solubility of ibrutinib in supercritical carbon dioxide (Sc-CO2): data correlation and thermodynamic analysis. *J. Chem. Thermodyn.* **182**, 107050 (2023).
61. Nasri, L. Modified Wilson's model for correlating solubilities in supercritical fluids of some polycyclic aromatic solutes. *Polycycl. Aromat. Compd.* **38**, 244–256 (2018).
62. Nasri, L., Bensaad, S. & Bensetiti, Z. Correlation and prediction of the solubility of solid solutes in chemically diverse supercritical fluids based on the expanded Liquid Theory. *Adv. Chem. Eng. Sci.* **3**, 255 (2013).
63. Nasri, L., Bensetiti, Z. & Bensaad, S. Correlation of the solubility of some Organic Aromatic pollutants in Supercritical Carbon Dioxide based on the UNIQUAC equation. *Energy Procedia*. **18**, 1261–1270. https://doi.org/10.1016/j.egypro.2012.05.142 (2012).
64. Gahtani, R. M., Talath, S., Hani, U., Rahmathulla, M. & Khalid, A. Pregabalin solubility in supercritical green solvent: a comprehensive experimental and theoretical-intelligent assessment. *J. Mol. Liq.*, **125339** (2024).

65. Hani, U. et al. Mathematical optimization and prediction of Febuxostat xanthine oxidase inhibitor solubility through supercritical CO2 system using machine-learning approach. *J. Mol. Liq.* **387**, 122486 (2023).
66. Marrero, J. & Gani, R. Group-contribution based estimation of pure component properties. *Fluid. Phase. Equilibria*. **183**, 183–208 (2001).
67. Klincewicz, K. & Reid, R. Estimation of critical properties with group contribution methods. *AIChE J.* **30**, 137–142 (1984).
68. Poling, B. E. & Prausnitz, J. M. & O'connell, J. P. The Properties of Gases and Liquids. Vol. 5 (Mcgraw-hill New York, (2001).
69. Madras, G., Kulkarni, C. & Modak, J. Modeling the solubilities of fatty acids in supercritical carbon dioxide. *Fluid. Phase. Equilibria*. **209**, 207–213 (2003).
70. Sodeifian, G., Razmimanesh, F., Sajadian, S. A. & Hazaveie, S. M. Experimental data and thermodynamic modeling of solubility of Sorafenib tosylate, as an anti-cancer drug, in supercritical carbon dioxide: evaluation of Wong-Sandler mixing rule. *J. Chem. Thermodyn.* **142**, 105998 (2020).
71. Sodeifian, G., Ardestani, N. S., Razmimanesh, F. & Sajadian, S. A. Experimental and thermodynamic analyses of supercritical CO2-Solubility of minoxidil as an antihypertensive drug. *Fluid. Phase. Equilibria*. **522**, 112745 (2020).
72. Majrashi, M. et al. Experimental measurement and thermodynamic modeling of Chlorothiazide solubility in supercritical carbon dioxide. *Case Stud. Therm. Eng.* **41**, 102621 (2023).
73. Sodeifian, G., Hazaveie, S. M. & Sajadian, S. A. Saadati Ardestani, N. Determination of the solubility of the repaglinide drug in supercritical carbon dioxide: experimental data and thermodynamic modeling. *J. Chem. Eng. Data*. **64**, 5338–5348 (2019).
74. Sodeifian, G., Razmimanesh, F. & Sajadian, S. A. Solubility measurement of a chemotherapeutic agent (Imatinib mesylate) in supercritical carbon dioxide: Assessment of new empirical model. *J. Supercrit Fluids*. **146**, 89–99. https://doi.org/10.1016/j.supflu.2019.01.006 (2019).
75. Sodeifian, G., Sajadian, S. A. & Ardestani, N. S. Determination of solubility of aprepitant (an antiemetic drug for chemotherapy) in supercritical carbon dioxide: empirical and thermodynamic models. *J. Supercrit. Fluids*. **128**, 102–111 (2017).
76. Esfandiari, N. & Sajadian, S. A. Solubility of Lacosamide in supercritical carbon Dioxide: an experimental analysis and thermodynamic modeling. *J. Mol. Liq.* **360**, 119467 (2022).
77. Tamura, K., Alwi, R. S., Tanaka, T. & Shimizu, K. Solubility of 1-aminoanthraquinone and 1-nitroanthraquinone in supercritical carbon dioxide. *J. Chem. Thermodyn.* **104**, 162–168 (2017).
78. Esfandiari, N. & Sajadian, S. A. Experimental and modeling investigation of glibenclamide solubility in supercritical carbon dioxide. *Fluid. Phase. Equilibria*. **556**, 113408. https://doi.org/10.1016/j.fluid.2022.113408 (2022).
79. Hazaveie, S. M., Sodeifian, G. & Sajadian, S. A. Measurement and thermodynamic modeling of solubility of Tamsulosin drug (anti cancer and anti-prostatic tumor activity) in supercritical carbon dioxide. *J. Supercrit. Fluids*. **163**, 104875 (2020).
80. Amani, M., Ardestani, N. S., Jouyban, A. & Sajadian, S. A. Solubility measurement of the fludrocortisone acetate in supercritical carbon dioxide: experimental and modeling assessments. *J. Supercrit. Fluids*. **190**, 105752. https://doi.org/10.1016/j.supflu.2022.105752 (2022).
81. Ardestani, N. S., Sajadian, S. A., Rojas, A., Alwi, R. S. & Estévez, L. A. Solubility of famotidine in supercritical carbon dioxide: experimental measurement and thermodynamic modeling. *J. Supercrit. Fluids*. **201**, 106031 (2023).
82. Sajadian, S. A., Amani, M., Ardestani, N. S. & Shirazian, S. Experimental analysis and thermodynamic modelling of lenalidomide solubility in supercritical carbon dioxide. *Arab. J. Chem.* **15**, 103821 (2022).
83. Sajadian, S. A., Ardestani, N. S., Esfandiari, N., Askarizadeh, M. & Jouyban, A. Solubility of favipiravir (as an anti-COVID-19) in supercritical carbon dioxide: an experimental analysis and thermodynamic modeling. *J. Supercrit. Fluids*. **183**, 105539 (2022).
84. Ansari, E., Honarvar, B., Sajadian, S. A., Aboosadi, Z. A. & Azizi, M. Experimental solubility of aripiprazole in supercritical carbon dioxide and modeling. *Sci. Rep.* **13**, 13402 (2023).
85. Sodeifian, G., Nateghi, H. & Razmimanesh, F. Measurement and modeling of dapagliflozin propanediol monohydrate (an anti-diabetes medicine) solubility in supercritical CO2: evaluation of new model. *J. CO2 Utilization*. **80**, 102687 (2024).
86. Sajadian, S. A., Esfandiari, N., Ardestani, S., Amani, N., Estévez, L. A. & M. & Measurement and modeling of the solubility of Mebeverine Hydrochloride in Supercritical Carbon Dioxide. *Chem. Eng. Technol.* **47**, 811–821 (2024).
87. Honarvar, B., Sajadian, S. A., Rojas, A., Galotto, M. J. & Jouyban, A. Solubility and thermodynamic modeling of sildenafil citrate in supercritical carbon dioxide. *Fluid. Phase. Equilibria*. **566**, 113677. https://doi.org/10.1016/j.fluid.2022.113677 (2023).
88. Sodeifian, G., Ardestani, N. S., Sajadian, S. A. & Panah, H. S. Experimental measurements and thermodynamic modeling of Coumarin-7 solid solubility in supercritical carbon dioxide: production of nanoparticles via RESS method. *Fluid Phase Equilib.* **483**, 122–143 (2019).
89. Wang, Y., Meng, T., Jia, D., Sun, Y. & Li, N. Solubility of Nifedipine and Lacidipine in Supercritical CO 2: measurement and correlation. *J. Solution Chem.* **46**, 70–88 (2017).
90. Martinez-Correa, H. A., Gomes, D. C. A., Kanehisa, S. L. & Cabral, F. A. Measurements and thermodynamic modeling of the solubility of squalene in supercritical carbon dioxide. *J. Food Eng.* **96**, 43–50 (2010).
91. Immirzi, A. & Perini, B. Prediction of density in organic crystals. *Acta Crystallogr. Sect. A*. **33**, 216–218 (1977).
92. Poling, B. E., Prausnitz, J. M., Paul, J. & Reid, O. C. *R.C. The Properties of Gases and Liquids* (McGraw-Hill, 2001).
93. Morales-Díaz, C., Cabrera, A. L., de la Fuente, J. C. & Mejía, A. Modelling of solubility of vitamin K3 derivatives in supercritical carbon dioxide using cubic and SAFT equations of state. *J. Supercrit. Fluids*. **167**, 105040. https://doi.org/10.1016/j.supflu.2020.105040 (2021).
94. Fedors, R. F. A method for estimating both the solubility parameters and molar volumes of liquids. *Polym. Eng. Sci.* **14**, 147–154 (1974).
95. Lee, B. I. & Kesler, M. G. A generalized thermodynamic correlation based on three-parameter corresponding states. *AIChE J.* **21**, 510–527 (1975).
96. Commerce, N. I. o. S. a. T. U. S. D. o. *NIST Chemistry WebBook*, https://webbook.nist.gov/chemistry/ (2018,October).
97. Guo, L., Qu, M., Jin, J. & Meng, H. Solubility of cinnamic acid in supercritical carbon dioxide and subcritical 1, 1, 1, 2-tetrafluoroethane: experimental data and modelling. *Fluid. Phase. Equilibria*. **480**, 66–80 (2019).
98. Pishnamazi, M. et al. Thermodynamic modelling and experimental validation of pharmaceutical solubility in supercritical solvent. *J. Mol. Liq.* **319**, 114120 (2020).
99. Pishnamazi, M. et al. Measuring solubility of a chemotherapy-anti cancer drug (busulfan) in supercritical carbon dioxide. *J. Mol. Liq.* **317**, 113954 (2020).
100. Pishnamazi, M. et al. Chloroquine (antimalaria medication with anti SARS-CoV activity) solubility in supercritical carbon dioxide. *J. Mol. Liq.* **322**, 114539 (2021).
101. Ongkasin, K., Sauceau, M., Masmoudi, Y., Fages, J. & Badens, E. Solubility of cefuroxime axetil in supercritical CO2: measurement and modeling. *J. Supercrit. Fluids*. **152**, 104498 (2019).
102. Shojaee, S. A., Rajaei, H., Hezave, A. Z., Lashkarbolooki, M. & Esmaeilzadeh, F. Experimental investigation and modeling of the solubility of carvedilol in supercritical carbon dioxide. *J. Supercrit. Fluids*. **81**, 42–47 (2013).
103. Ahmadi Sabegh, M., Rajaei, H., Zeinolabedini Hezave, A. & Esmaeilzadeh, F. Amoxicillin solubility and supercritical carbon dioxide. *J. Chem. Eng. Data*. **57**, 2750–2755 (2012).
104. Nasri, L. About consistency of Solid's solubility data in supercritical CO2 and some thermodynamic properties estimation. *Sustainable Chem. Pharm.* **13**, 100145 (2019).
105. Coimbra, P., Gil, M., Duarte, C., Heron, B. M. & De Sousa, H. Solubility of a spiroindolinonaphthoxazine photochromic dye in supercritical carbon dioxide: experimental determination and correlation. *Fluid. Phase. Equilibria*. **238**, 120–128 (2005).

106. Huang, Z., Yang, X. W., Sun, G. B., Song, S. W. & Kawi, S. The solubilities of xanthone and xanthene in supercritical carbon dioxide: structure effect. *J. Supercrit. Fluids*. **36**, 91–97 (2005).
107. Khimeche, K., Alessi, P., Kikic, I. & Dahmani, A. Solubility of diamines in supercritical carbon dioxide: experimental determination and correlation. *J. Supercrit. Fluids*. **41**, 10–19 (2007).

Acknowledgment

The authors extend their appreciation to the Deanship of Scientific Research at King Khalid University for funding this work through a Large group Research Project under grant number RGP.2/21/45.

Author contributions

A.F.W.: writing, editing, formal analysis, validationS.B.S.: writing, editing, analysis, evaluation, resourcesS.T.: writing, editing, investigation, analysisJ.R.P.: writing, editing, formal analysis, validationJ.S.: writing, editing, analysis, evaluation, resourcesM.B.: writing, editing, formal analysis, validationB.K.M.: U.H.: writing, editing, formal analysis, validation, supervision.

Declarations

Competing interests

The authors declare no competing interests.

Additional information

Correspondence and requests for materials should be addressed to U.H.

Reprints and permissions information is available at www.nature.com/reprints.

Publisher's note Springer Nature remains neutral with regard to jurisdictional claims in published maps and institutional affiliations.